# Enhanced nonreciprocal radiation in Weyl semimetals by attenuated total reflection

Xiaohu Wu, Haiyan Yu, Feng Wu, et al.

**COLLECTIONS**

This paper was selected as an Editor's Pick

View Online     Export Citation     CrossMark

---

**ARTICLES YOU MAY BE INTERESTED IN**

Nonreciprocal thermal radiation of nanoparticles via spin-directional coupling with reciprocal surface modes
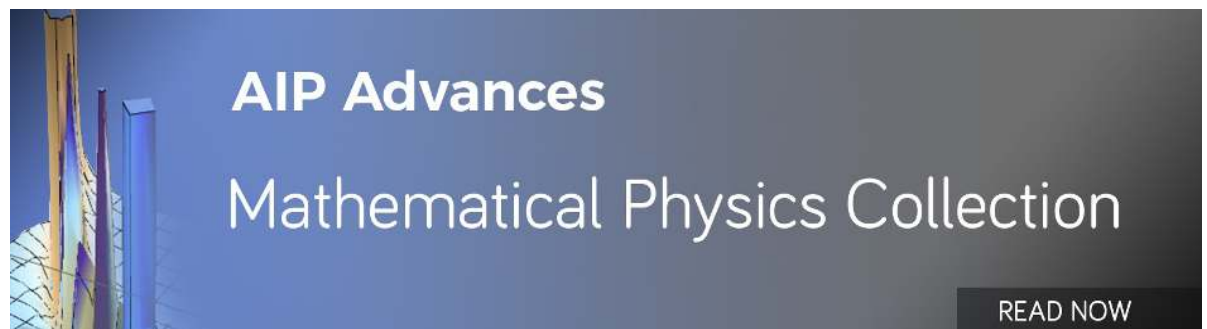Applied Physics Letters **119**, 021104 (2021); https://doi.org/10.1063/5.0057446

Nonreciprocal photonic spin Hall effect of magnetic Weyl semimetals
Applied Physics Letters **119**, 081103 (2021); https://doi.org/10.1063/5.0059792

Tunable GH shifts in Weyl thin films on a Weyl substrate
Journal of Applied Physics **129**, 153103 (2021); https://doi.org/10.1063/5.0043579

**AIP Advances**
Mathematical Physics Collection
READ NOW

# Enhanced nonreciprocal radiation in Weyl semimetals by attenuated total reflection (EP)

View Online    Export Citation    CrossMark

Xiaohu Wu,[1,a]  (iD)  Haiyan Yu,[1]  Feng Wu,[2]  (iD)  and Biyuan Wu[1,3]

## AFFILIATIONS

[1] Shandong Institute of Advanced Technology, Jinan 250100, China
[2] School of Optoelectronic Engineering, Guangdong Polytechnic Normal University, Guangzhou 510665, China
[3] School of Automation and Information Engineering, Xi'an University of Technology, Xi'an, Shaanxi 710048, China

[a] Author to whom correspondence should be addressed: xiaohu.wu@iat.cn

## ABSTRACT

Recent studies have suggested that Weyl semimetals were the promising materials to verify Kirchhoff's law for nonreciprocal materials in experiment. Nevertheless, existing designs based on Weyl semimetals could not achieve perfect nonreciprocal radiation around a wavelength of 10 $\mu$m at small angles. Therefore, it is of significant importance to design structures that can realize perfect nonreciprocal radiation at a shorter wavelength and smaller angle. Here, by using attenuated total reflection, we demonstrate that perfect nonreciprocal radiation can be realized at a wavelength of 10 $\mu$m at an angle of 30°. The difference between directional emissivity and absorptivity is as large as 0.99, which is the best result until now, as far as we know. The perfect nonreciprocal radiation is attributed to the nonreciprocal guided resonances in the Weyl semimetal film, which is confirmed by the distribution of magnetic field and dispersion relation. Such a design is promising in verifying Kirchhoff's law for nonreciprocal materials in experiment.

## I. INTRODUCTION

It has been long recognized in the literature that most thermal emitters obey the traditional Kirchhoff's law, which states that the direction emissivity and absorptivity are equal.[1–3] However, recent studies suggested that the traditional Kirchhoff's law only holds for reciprocal materials, but not nonreciprocal materials, which do not obey Lorentz reciprocity.[4–12] The nonreciprocal radiation (NRR), which occurs in nonreciprocal materials, provides new opportunities in energy harvesting and infrared camouflage.[7,13] Zhang et al. generalized the traditional Kirchhoff's law to make it hold for both reciprocal and nonreciprocal materials.[14] The generalized Kirchhoff's law equals to the traditional Kirchhoff's law for reciprocal materials, and they are different for nonreciprocal materials. Until now, Kirchhoff's law for nonreciprocal materials, which is of great importance in thermal radiation, has not been verified in experiment.

To verify Kirchhoff's law for nonreciprocal materials, the emissivity and absorptivity should be measured directly. With current measurement technologies, it is possible to accurately measure the emissivity and absorptivity at wavelength smaller than and around 10 $\mu$m.[15–19] Both gyrotropic materials and Weyl semimetals can break Lorentz reciprocity, in which NRR can be realized.[4–12] Conventional gyrotropic materials possess weak magneto-optical effect in mid-infrared band with external magnetic field.[4–9,20–22] Even though strong NRR can be realized around a wavelength of 10 $\mu$m, the external magnetic field should be as large as 3 T, which is unfavorable to experiment.[7] On the other hand, the Weyl semimetals are the most promising materials since they possess intrinsic nonreciprocity without external magnetic field.[10–12] However, existing structures based on them could only realize perfect NRR around a wavelength of 15 $\mu$m, and the angle is as large as 60°.[10–12] In addition, according to Lambert's cosine law, the emitted energy of any object is smaller at larger angles. Thus, it is desirable to design structure that can realize perfect NRR near a wavelength of 10 $\mu$m at small angles. The nonreciprocity of Weyl semimetals has not been fully investigated and should be explored further.[23–25]

In this work, by using attenuated total reflection, we demonstrate that perfect NRR can be realized in a planar Weyl semimetal film. Specifically, the difference between directional emissivity and

absorptivity can be as large as 0.99 at a wavelength of 10 $\mu m$ at an angle of 30°. We believe that such a design is promising in verifying Kirchhoff's law for nonreciprocal materials in experiment.

## II. MODELING

As shown in Fig. 1, the Weyl semimetal film with thickness $d_2$ is on the top of a uniform silver (Ag) layer acting as a mirror. The thickness of the Ag layer is 0.2 $\mu m$, which is optically thick. The prism is chosen with a relatively large refractive index so that it can provide a larger wavevector to couple the incident light with the guided resonances inside the Weyl semimetal.[26] Here, we consider a diamond prism with permittivity $\varepsilon_p$ = 5.5.[27] The thickness of the air gap between the prism and Weyl semimetal film is denoted by $d_1$. The permittivity of Ag is described by the Drude model.[28] The wavevector along the $x$-axis provided by the prism is $k_x = \sqrt{\varepsilon_p} \sin \theta k_0$, where $k_0$ is the wavevector in the vacuum and $\theta$ is the angle of incidence.

In Weyl semimetals, the time-reversal symmetry needs to be broken to split a doubly degenerate Dirac point a pair of Weyl nodes with opposite chirality. Each pair of Weyl nodes is separated in momentum space (denoted by wave vector 2b) by breaking time-reversal symmetry. The presence of Weyl nodes changes the electromagnetic response, and the displacement electric field for Weyl semimetals can be written as[10]

$$\mathbf{D} = \varepsilon_d \mathbf{E} + \frac{ie^2}{4\pi^2 \hbar \omega}(-2b_0 \mathbf{B} + 2\mathbf{b} \times \mathbf{E}). \qquad (1)$$

Here, $\varepsilon_d$ is the permittivity of the corresponding Dirac semimetal, which has doubly degenerate bands with $b_0 = \mathbf{b} = 0$. Below, we assume $\varepsilon_d$ is isotropic. The first and the second terms in Eq. (1) describe the chiral magnetic effect and the anomalous Hall effect, respectively. In this paper, we consider only materials where the Weyl nodes have the same energy (i.e., $b_0 = 0$). Considering 2b along the z-direction (i.e., $\mathbf{b} = b\hat{z}$), the permittivity tensor of the Weyl semimetal becomes[10]

$$\boldsymbol{\varepsilon} = \begin{bmatrix} \varepsilon_d & 0 & -j\varepsilon_a \\ 0 & \varepsilon_d & 0 \\ j\varepsilon_a & 0 & \varepsilon_d \end{bmatrix}, \qquad (2)$$

where

$$\varepsilon_a = \frac{be^2}{2\pi^2 \hbar \omega}. \qquad (3)$$

Since $b \neq 0$, $\varepsilon_a$ becomes nonzero; therefore, the permittivity tensor is asymmetric and breaks Lorentz reciprocity. The diagonal term $\varepsilon_d$ is calculated by using the Kubo–Greenwood formalism within the random phase approximation to a two-band model with spin degeneracy. The explicit expression can be found in Ref. 10.

To compared with the results in Ref. 10, here the parameters of the Weyl semimetal are the same to those in Ref. 10. At the temperature 300 K, we plot $\varepsilon_a$ and $\varepsilon_d$ as functions of wavelength, as shown in Fig. 2. The real part of $\varepsilon_d$ is negative as the wavelength is larger than 8.63 $\mu m$. Besides, we have verified that the permittivity tensor calculated in this work is consistent with that calculated from Ref. 10.

We consider the transverse magnetic (TM) wave with electric fields in the $x$–$z$ plane, and thus, there is no polarization conversion between two linearly polarized waves. For a homogeneous material filling a half-space, and the radiation exchanged through a surface element with a blackbody radiator at the same temperature under angles $\theta$ and $-\theta$, conservation of energy and detailed balance led to[20]

$$\alpha(\theta) + R(\theta) = \alpha(-\theta) + R(-\theta) = 1. \qquad (4)$$

The second law of thermodynamics demands that[20]

$$e(-\theta) + R(\theta) = e(\theta) + R(-\theta) = 1, \qquad (5)$$

where $R$, $\alpha$, and $\varepsilon$ are reflectivity, absorptivity, and emissivity, respectively. According to Eqs. (4) and (5), one can get the absorptivity and emissivity, respectively,
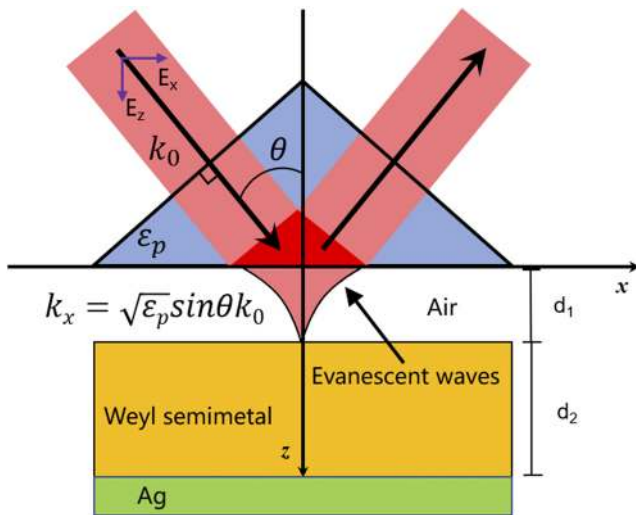


FIG. 1. Geometry of attenuated total reflection off the Weyl semimetal surface. The plane of incidence is the $x$–$z$ plane, and the thicknesses of the air gap and the Weyl semimetal film are $d_1$ and $d_2$, respectively. The silver substrate is optically thick. The electric field is in the $x$–$z$ plane, while the magnetic field is along the $y$-axis. The angle of incidence is $\theta$, and the permittivity of the prism is $\varepsilon_p$.
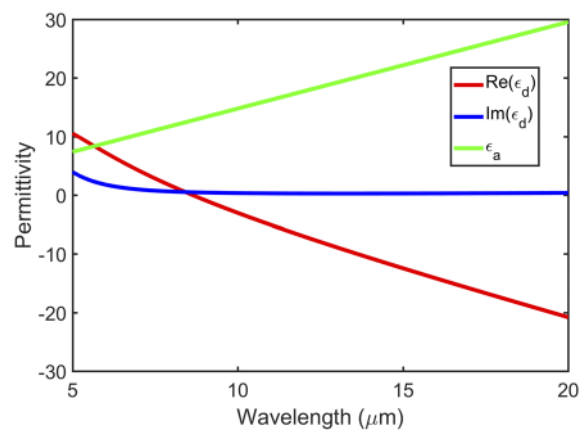


FIG. 2. Components of the permittivity tensor of the Weyl semimetal.

$$\alpha(\theta) = 1 - R(\theta) \tag{6}$$

and

$$e(\theta) = 1 - R(-\theta). \tag{7}$$

The difference between emissivity and absorptivity is defined as $\eta(\theta) = |e(\theta) - \alpha(\theta)|$, measuring the nonreciprocal radiation. According to Eqs. (4) and (5), the nonreciprocal radiation is identical for angles of $\theta$ and $-\theta$.

Besides, once the reflectivity is obtained, the absorptivity, emissivity, and nonreciprocal radiation can be calculated. The reflectivity can be calculated by the standard transfer matrix method.[29–32] Taking one Weyl semimetal film with thickness $d_2$, for example, we introduce the transfer matrix method. The electromagnetic fields in the Weyl semimetal can be expressed as

$$\mathbf{H} = \mathbf{U}(z) \exp(j\omega t - jk_x x), \text{ where } \mathbf{U} = (0, U_y, 0), \tag{8}$$

and

$$\mathbf{E} = j(\mu_0/\varepsilon_0)^{1/2}\mathbf{S}(z) \exp(j\omega t - jk_x x), \text{ where } \mathbf{S} = (S_x, 0, S_z). \tag{9}$$

Note that $\varepsilon_0$ and $\mu_0$ are the absolute permittivity and permeability of vacuum, respectively, and $\omega$ is the angular frequency. By substituting Eqs. (8) and (9) into Maxwell's equations and setting $K_x = k_x/k_0$, we obtain the following differential equations:

$$\frac{\partial}{\partial z}\begin{pmatrix} U_y \\ S_x \end{pmatrix} = k_0 \begin{bmatrix} \varepsilon_a/\varepsilon_d K_x & \varepsilon_d - \varepsilon_a^2/\varepsilon_d \\ K_a^2/\varepsilon_d - 1 & -\varepsilon_a/\varepsilon_d K_x \end{bmatrix}\begin{pmatrix} U_y \\ S_x \end{pmatrix}. \tag{10}$$

The electromagnetic fields in the Weyl semimetal film can be described by the eigenvalues and eigenvectors of the coefficient matrix. The electromagnetic fields in the Weyl semimetal with thickness $d_2$ can be expressed as

$$U_y(z) = w_{11}c_1 \exp(k_0 q_1 z) + w_{12}c_2 \exp(k_0 q_2(z - d_2)), \tag{11}$$

$$S_x(z) = w_{21}c_1 \exp(k_0 q_1 z) + w_{22}c_2 \exp(k_0 q_2(z - d_2)), \tag{12}$$

where $w_{im}$ is the corresponding element of the eigenvector matrix $\mathbf{W}$ of the coefficient matrix in Eq. (10), $q_1$ and $q_2$ are the two eigenvalues of matrix $\mathbf{A}$ with the negative real part and positive real part, respectively, and $c_1$ and $c_2$ are unknowns. By applying the boundary conditions, i.e., the tangential components of the magnetic and electric field vectors should be continuous at the interface, it can be shown that

$$\begin{pmatrix} 1 \\ -jZ \end{pmatrix} + \begin{pmatrix} 1 \\ jZ \end{pmatrix}r = \mathbf{W}\begin{pmatrix} 1 & 0 \\ 0 & \exp(-k_0 q_2 d_2) \end{pmatrix}\begin{pmatrix} c_1 \\ c_2 \end{pmatrix}, \tag{13}$$

$$\mathbf{W}\begin{pmatrix} 1 & 0 \\ 0 & \exp(k_0 q_1 d_2) \end{pmatrix}\begin{pmatrix} c_1 \\ c_2 \end{pmatrix} = \begin{pmatrix} 1 \\ -jZ \end{pmatrix}t, \tag{14}$$

where $Z = \sin\theta/n_1$, $n_1$ is the refractive index of the incident medium, and $r$ and $t$ are the reflection and transmission coefficients, respectively. From Eqs. (13) and (14), the reflection coefficient can be obtained. The reflection is $R = |r|^2$. The transfer matrix method can be expended for multilayer structures, and the detailed information can be found in Refs. 29–32.

## III. RESULTS AND DISCUSSIONS

According to Planck's law, the blackbody emits the largest energy at wavelength around 10 $\mu$m when the temperature is 300 K. Hence, we first investigate the emissivity and absorptivity at 10 $\mu$m. The emissivity and absorptivity varying with $d_1$ and $d_2$ are shown in Figs. 3(a) and 3(b), respectively. The difference between them is also shown in Fig. 3(c). The angle of incidence is 30°, which is much smaller than that in Refs. 10 and 12. One can see that perfect emissivity can occur in Fig. 3(a), while the absorptivity in Fig. 3(b) is smaller. As a result, the emissivity and absorptivity can be significantly different, resulting in completely violating the traditional Kirchhoff's law. Besides, it is clear that the emissivity is not much sensitive to the thickness of the air gap. The underlying mechanism will be verified by showing the distribution of magnetic field and investigating the dispersion relation in the following.

The proper choice of the thicknesses can be obtained from Fig. 3(c). When the thicknesses of the air gap and Weyl semimetal film are 2.02 and 0.137 $\mu$m, respectively, the absorptivity and emissivity spectra at an angle of 30° are shown in Fig. 4. At a wavelength of 10 $\mu$m, the emissivity can reach 0.999, while the absorptivity can be as small as 0.007, and thus, the difference between them is 0.992. As far as we know, it is the biggest difference between emissivity and absorptivity until now.

To understand the mechanism for enhanced nonreciprocal radiation, we discuss the possibility of the excitation of the surface plasmon polaritons, which has been used to enhance the nonreciprocal radiation in the Weyl semimetal film.[10] The z-component of the wavevector in the Weyl semimetal is $k_{z2} = \sqrt{\varepsilon_v k_0^2 - k_x^2}$, where $\varepsilon_v = \varepsilon_d - \varepsilon_a^2/\varepsilon_d$. At a wavelength of 10 $\mu$m, there is $\varepsilon_d = -3.03 + 0.34j$ and $\varepsilon_a = 14.78$. Therefore, the electromagnetic waves in the Weyl semimetal film are propagating waves, rather than evanescent waves. Thus, the surface plasmon polaritons cannot be excited in this case, which is different from the previous study.[10] Because the electromagnetic waves in the air gap and Ag substrate are evanescent waves, these are guided resonances excited in the Weyl semimetal film. To
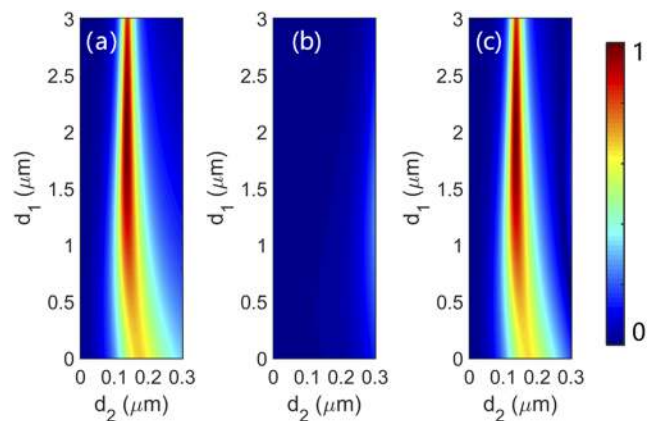
**FIG. 3.** (a) Emissivity and (b) absorptivity as a function of the thicknesses of the air gap and the Weyl semimetal. (c) Difference between the emissivity and the absorptivity as a function of the thicknesses of the air gap and the Weyl semimetal. The angle of incidence is 30°. The wavelength is 10 $\mu$m.
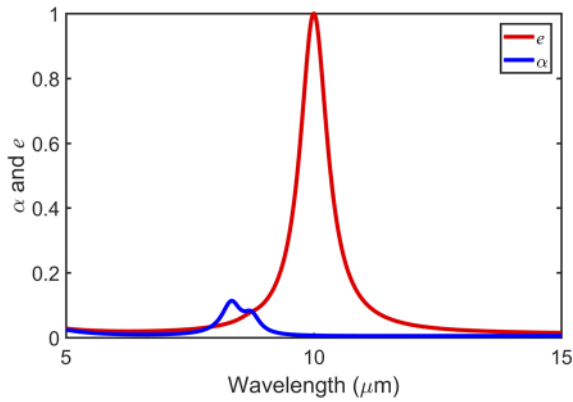
**FIG. 4.** Emissivity and absorptivity as a function of wavelength. The angle of incidence is 30°. The thicknesses of the air gap and Weyl semimetal film are 2.02 and 0.137 $\mu$m, respectively.

confirm the exciting of guided resonance, its dispersion relation can be calculated from[4]

$$\tan(k_{z2}d_2) = \frac{\varepsilon_d k_{z2} k_{z1}}{\varepsilon_d k_0^2 - k_x^2 - \varepsilon_a k_x k_{z1}}, \quad (15)$$

where $k_{z1} = \sqrt{k_0^2 - k_x^2}$ describes the exponential decay of the fields in vacuum. At a wavelength of 10 $\mu$m, Eq. (15) can be roughly satisfied at an angle of incidence of −30°, indicating that there is the excitation of guided resonances, and it is the reason for the weak reflectivity. However, Eq. (15) cannot be satisfied at an angle of incidence of 30°, and it is the reason for weak absorptivity. Therefore, the strong nonreciprocal radiation stems from the nonreciprocal guided resonances.

To further investigate the mechanism, the distribution of the absolute of the magnetic field along the $y$-axis is also plotted. Figure 5(a) shows the results at a wavelength of 10 $\mu$m for angles of incidence of −30° and 30°. The magnitude of the incident magnetic field is set to unity. For an angle of incidence of −30°, the magnetic field is greatly enhanced in the interface between Weyl semimetal and Ag, resulting in perfect absorption and small reflection. According to Eq. (3), the emissivity is very weak at angle of 30°. In contrast, for an angle of incidence of 30°, the magnetic field in the interface between Weyl semimetal and Ag is much weaker, indicating that most of the incident power is reflected, resulting in a low absorptivity. Therefore, the perfect NRR is attributed to the nonreciprocal guided resonances excited in the Weyl semimetal film, which can be verified by the magnetic field distribution. In addition, the distribution of the magnetic field is shown in Fig. 5(b) when there is no air gap between the prism and the Weyl semimetal film. In this case, the difference in the magnetic field for angles of incidence of −30° and 30° is smaller than that shown in Fig. 5(a). Therefore, the nonreciprocity is weaker in this case. The magnetic field distribution can well explain the results shown in Fig. 3(a).

The emissivity and absorptivity as functions of the angle of incidence are shown in Fig. 6. One can see that the nonreciprocal radiation occurs around an angle of incidence of 30°. When the angle of incidence is larger than 60°, both the emissivity and absorptivity are
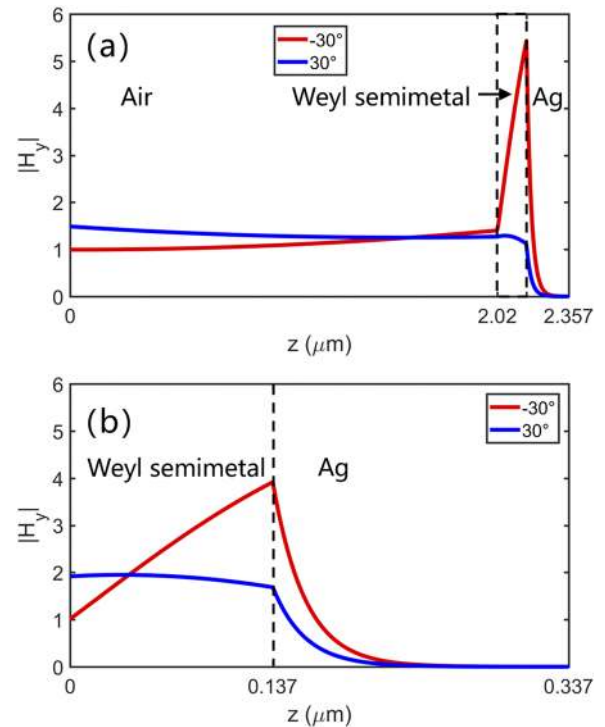


**FIG. 5.** The distribution of the absolute of the magnetic field along the y-axis at a wavelength of 10 $\mu$m when the angles of incidence are −30° and 30°. The dashed black lines indicate the interfaces. (a) The thickness of the air gap is 2.02 $\mu$m, and the thickness of the Weyl semimetal film is 0.137 $\mu$m. (b) There is no air gap between the prism and the Weyl semimetal film, and the thickness of the Weyl semimetal film is 0.137 $\mu$m. The magnitude of the incident magnetic field is set to unity.

close to zero. When the angle of incidence is smaller than 60°, the emissivity is always larger than the absorptivity.

In experiment, the emissivity and absorptivity of the proposed structure shown in Fig. 1 should be directly measured. It is noted that
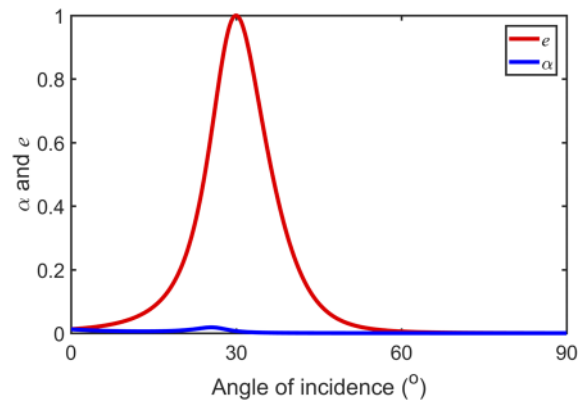


**FIG. 6.** Emissivity and absorptivity as functions of the angle of incidence. The wavelength is 10 $\mu$m. The thicknesses of the air gap and Weyl semimetal film are 2.02 and 0.137 $\mu$m, respectively.

the direct measurement of the emissivity spectra of quartz and amorphous has been successfully operated with the existing of a prism.[33] Therefore, the adding of the prism should not be a problem in the measurement.

It is noted that the absorptivity is asymmetry in this work. Previous studies have shown that in reciprocal materials, such as quartz crystal, asymmetry absorptivity can also be obtained.[34–36] It should be emphasized that the focus of this work is the difference between emissivity and absorptivity, rather than asymmetric absorptivity. Nonreciprocal radiation cannot be achieved with reciprocal materials since they do not break the Lorentz reciprocity. Besides, hyperbolic antiferromagnets, which break Lorentz reciprocity, have been studies to achieve asymmetry reflectivity.[37] Such materials are promising to realize strong nonreciprocal radiation. As far as we know, Weyl semimetals are the most promising candidates for realizing nonreciprocal radiation because they do not need external magnetic field.

## IV. CONCLUSIONS

In summary, by using attenuation total reflection, we demonstrated that the perfect nonreciprocal radiation at a wavelength of 10 $\mu$m at an angle of 30° could be realized. The difference between directional emissivity and absorptivity can be as large as 0.99, which is the best result until now, as far as we know. The perfect nonreciprocal radiation is attributed to the nonreciprocal guided resonances excited in the Weyl semimetal film, which is confirmed by the magnetic field distribution and the dispersion relation. Such a design is promising to be utilized to verify Kirchhoff's law for nonreciprocal materials.

## ACKNOWLEDGMENTS

## DATA AVAILABILITY

The data that support the findings of this study are available within the article.

## REFERENCES

[1] G. Kirchhoff, Philos. Mag. Ser. **20**, 1–21 (1860).
[2] Z. M. Zhang, *Nano/Microscale Heat Transfer* (McGraw-Hill, 2007).
[3] X. H. Wu, *Thermal Radiative Properties of Uniaxial Anisotropic Materials and Their Manipulations* (Springer Singapore, 2021).
[4] L. Zhu and S. H. Fan, Phys. Rev. B **90**, 220301 (2014).
[5] B. Zhao, Y. Shi, J. Wang, Z. Zhao, N. Zhao, and S. Fan, Opt. Lett. **44**, 4203 (2019).
[6] X. H. Wu, ES Energy Environ. **12**, 46–51 (2021).
[7] X. H. Wu, Z. X. Chen, and F. Wu, ES Energy Environ. (published online 2021).
[8] J. Dong, W. Zhang, and L. Liu, J. Quant. Spectrosc. Radiat. Transfer **255**, 107279 (2020).
[9] A. Caratenuto, Y. Tian, M. Antezza, G. Xiao, and Y. Zheng, arXiv:2101.05852.
[10] B. Zhao, C. Guo, C. A. C. Garcia, P. Narang, and S. H. Fan, Nano Lett. **20**, 1923–1927 (2020).
[11] Y. Tsurimaki, X. Qian, S. Pajovic, F. Han, M. Li, and G. Chen, Phys. Rev. B **101**, 165426 (2020).
[12] S. Pajovic, Y. Tsurimaki, X. Qian, and G. Chen, Phys. Rev. B **102**, 165417 (2020).
[13] M. A. Green, Nano Lett. **12**, 5985–5988 (2012).
[14] Z. M. Zhang, X. H. Wu, and C. J. Fu, J. Quant. Spectrosc. Radiat. Transfer **245**, 106904 (2020).
[15] Z. M. Zhang and L. P. Wang, Int. J. Thermophys. **34**, 2209–2242 (2013).
[16] T. R. Fu, Y. Xiong, J. Liu, and C. Shi, J. Heat Transfer **141**, 082702 (2019).
[17] L. P. Wang and Z. M. Zhang, J. Heat Transfer **135**, 091505 (2013).
[18] Y. Xiao, C. Wan, A. Shahsafi, J. Salman, Z. Yu, R. Wambold, H. Mei, B. E. R. Perez, W. Derdeyn, C. Yao, and M. A. Kats, Laser Photonics Rev. **14**, 1900443 (2020).
[19] Y. Xiao, A. Shahsafi, C. Wan, P. J. Roney, G. Joe, Z. Yu, J. Salman, and M. A. Kats, Phys. Rev. Appl. **11**, 014026 (2019).
[20] L. Remer, E. Mohler, W. Grill, and B. Lüthi, Phys. Rev. B **30**, 3277 (1984).
[21] N. Liu, J. Zhao, L. Du, C. Niu, X. Lin, Z. Wang, and X. Li, Opt. Lett. **44**, 3050–3053 (2019).
[22] N. Liu, J. Zhao, L. Du, C. Niu, C. Sun, X. Kong, Z. Wang, and X. Li, Opt. Lett. **45**, 5917–5920 (2020).
[23] T. Tamaya, T. Kato, K. Tsuchikawa, S. Konabe, and S. Kawabata, J. Phys.: Condens. Matter **31**, 305001 (2019).
[24] K. Halterman, M. Alidoust, and A. Zyuzin, Phys. Rev. B **98**, 085109 (2018).
[25] K. Tsuchikawa, S. Konabe, T. Yamamoto, and S. Kawabata, Phys. Rev. B **102**, 035443 (2020).
[26] K. Halterman and M. Alidoust, Opt. Express **27**, 36164–36182 (2019).
[27] R. Macêdo, T. Dumelow, R. E. Camley, and R. L. Stamps, ACS Photonics **5**, 5086–5094 (2018).
[28] X. H. Wu and C. J. Fu, AIP Adv. **7**, 075208 (2017).
[29] J. J. Wang, Y. R. Zhang, and Y. T. Fang, J. Nanophotonics **8**, 084099 (2014).
[30] Y.-T. Fang, L. Han, and Y.-F. Gao, Z. Naturforsch. **70**, 205–211 (2015).
[31] R. Macêdo, Solid State Phys. **68**, 91–155 (2017).
[32] Z. Guo, F. Wu, C. Xue, H. Jiang, Y. Sun, Y. Li, and H. Chen, J. Appl. Phys. **124**, 103104 (2018).
[33] S. Zare, C. P. Tripp, and S. Edalatpour, Phys. Rev. B **100**, 235450 (2019).
[34] F. Wu and X. H. Wu, J. Opt. Soc. Am. B **38**, 1452–1456 (2021).
[35] R. Macêdo, C. A. McEleney, M. González-Jiménez, and X. H. Wu, Opt. Photonics News **31**, 53 (2020).
[36] X. H. Wu, C. A. McEleney, M. González-Jiménez, and R. Macêdo, Optica **6**, 1478–1483 (2019).
[37] R. Macedo and R. E. Camley, Phys. Rev. B **99**, 014437 (2019).